NATIONAL ADVISORY COMMITTEE
FOR AERONAUTICS

TECHNICAL NOTE

No. 1776

HYDRODYNAMIC IMPACT LOADS IN ROUGH WATER FOR A PRISMATIC

FLOAT HAVING AN ANGLE OF DEAD RISE OF 30°

By Robert W. Miller

Langley Aeronautical Laboratory
Langley Field, Va.

NACA

Washington

December 1948
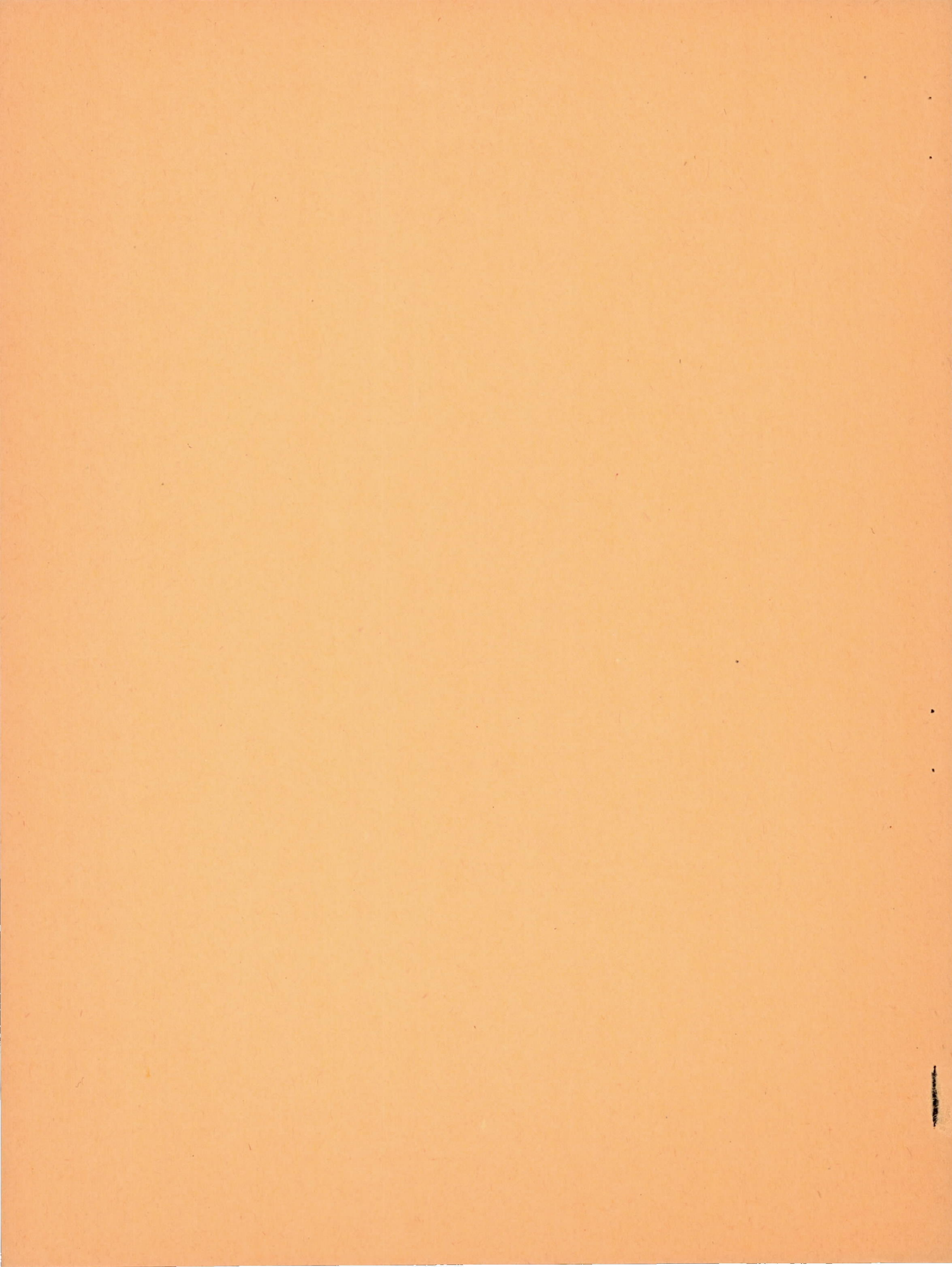
NATIONAL ADVISORY COMMITTEE FOR AERONAUTICS

TECHNICAL NOTE NO. 1776

HYDRODYNAMIC IMPACT LOADS IN ROUGH WATER FOR A PRISMATIC

FLOAT HAVING AN ANGLE OF DEAD RISE OF 30°

By Robert W. Miller

SUMMARY

An investigation was conducted in the Langley impact basin to
determine the hydrodynamic impact loads in rough water for a prismatic-
float forebody having an angle of dead rise of 30°. The test runs were
made at fixed trim and each impact occurred into an advancing wave
2 feet in height and 60, 45, or 30 feet in length.

Analysis of the data has shown that if the maximum slope of a
comparable trochoid is used in the hydrodynamic-load equation for the
calculation of rough-water loads, the calculated values of maximum load
agree with the measured loads within 10 percent for waves longer than
5 float-forebody lengths, that a relationship exists between the wave
slope and the slope of an equivalent inclined-plane water surface for
any point of contact, and that airplanes designed for hard, high-flight-
path-angle impacts in smooth water can be used safely for landings in
rough water at low speeds and flight-path angles.

INTRODUCTION

In order to obtain the maximum utility from some types of seaplanes
or flying boats, they must be able to operate from undeveloped and
unprotected landing areas and under adverse sea conditions. The problem
of designing an airplane capable of fulfilling such requirements has been
complicated by the lack of adequate data on the loads encountered in
rough-water impacts.

This paper gives data on the loads for a prismatic-float forebody
having an angle of dead rise of 30° encountered in impacts against various
portions of an advancing wave. A method of applying theories derived
for smooth-water conditions to the rough-water case is also discussed,
and rough-water load results are compared with calculated smooth-water
values.

In presenting the data an effort has been made to correlate the
experimental results in rough water with calculated values obtained by

the application of smooth-water hydrodynamic impact theory under the
assumption that the wave surface may be simulated by an inclined-plane
water surface, as suggested in references 1 and 2. In reference 2,
theoretical loads calculated on this basis for a scalloped-bottom float
were shown to be in fair agreement with the results of some rough-water
impacts. This paper reports the results of a much larger number of
rough-water tests and compares the results with calculated values.

SYMBOLS

A aspect ratio $\left(\tan\beta/\tan\tau\right)$

C_l maximum impact-load-factor coefficient

g acceleration due to gravity, feet per second per second

H wave height measured from trough to crest, feet

L wave length measured from crest to crest, feet

n_i maximum impact load factor

V velocity, feet per second

W dropping weight, pounds

X horizontal distance from previous crest, feet

Y vertical distance of a point in water surface from
             midheight between trough and crest, feet

β angle of dead rise, radians except where otherwise noted

γ flight-path angle, degrees

θ angle of inclination of water surface, degrees

κ approach parameter

ρ mass density of fluid, slugs per cubic foot

τ trim, degrees

$f(\beta)$ dead-rise variation

$\phi(A)$ aspect-ratio (end flow) correction

Subscripts:

e   effective (referred to inclined water surface)

f   float

h   horizontal direction

m   measured

n   normal to plane of inclined water surface

o   initial time (contact)

r   resultant

th   computed by use of theory

v   vertical direction

w   wave

Any other consistent system of units may be used.

APPARATUS

Basin.- The Langley impact basin and standard equipment used are described in reference 3.

Model.- The model was a prismatic-float forebody 10 feet in length having an angle of dead rise of 30° and a test weight of about 1230 pounds. The principal lines and dimensions defining the shape and size of the model are shown in figure 1 and the offsets are given in table I.

Instrumentation.- The instruments used to measure the displacement and velocity in both the horizontal and vertical directions are described in reference 3. Accelerations in the vertical direction were measured by two standard NACA accelerometers having natural frequencies of 21 and 26 cycles per second with approximately 0.67 critical damping. Wave profiles were measured by photographing the water surface against a scale painted on the basin wall.

Wave maker.- The rough-water conditions required for the tests were provided by the Langley impact-basin wave maker (fig. 2) which was designed to generate waves up to 60 feet in length and 3 feet in

height. Somewhat longer waves of less height or shorter waves of more
height can be produced. The waves proceed from the wave maker through
the test section and then break on a sloping beach designed to minimize
reflected waves.

The prime mover of the wave-maker system is an internal-combustion
engine with a constant-speed device. The rotary motion of this engine,
operating through a speed-reduction gear, is transformed into recipro-
cating motion by a double-throw eccentric, which is adjustable to any
double amplitude from 0 to 24 inches. The reciprocating motion is then
transmitted by a system of bell cranks, shafting, and connecting rods to
the wave generator.

The wave generator is a plate occupying the full width and depth
of the basin and is suspended by hangers from the upper part of the
building. In order to approximate the motion of the water particles
in a shallow-water wave, the plate is given the motion of a segment of
a plane rotating about a horizontal axis located beneath the floor of
the basin, as indicated by the small sketch in the upper right-hand
corner of figure 2. Adjustment of the relative amplitudes of the upper
and lower portions of the plate, which is accomplished by means of a
change in setting of the first bell crank, permits the required motion
of this type for a wide range of wave sizes and forms.

In order to obtain impacts on desired portions of the wave profile,
the float motion must be correlated with the wave motion. This correla-
tion is accomplished by means of a switch attached to the wave-maker
activating mechanism which, when the waves have attained the desired
size and form, first starts the carriage instrumentation and then, at
the proper point in its cycle, fires the catapult gun. The float there-
fore begins its run at such a time that the horizontal and vertical
motions bring it to the desired point of impact at the instant the
proper portion of the wave reaches the same point.

PRECISION

The apparatus and instrumentation used in the tests give measure-
ments which are believed to be accurate within the following limits:

Horizontal velocity, feet per second . . . . ±0.5
Vertical velocity, feet per second . . . . ±0.2
Weight, pounds . . . . ±2.0
Acceleration, g, percent of reading . . . . 0 to -10
Vertical displacement of point of contact, feet . . . . ±0.05

TEST PROCEDURE

The test program was carried out in the Langley impact basin with each impact occurring on a wave traveling in a direction opposite to that of the float (fig. 3). The waves used in the tests were 60, 45, or 30 feet in length but were all about 2 feet in height and of a shape similar to the profiles shown in figure 4. The wave slopes as measured from these profiles are compared in figures 5 and 6 with the slopes of trochoidal waves of dimensions similar to those of the tests.

The test runs were made with the float set at fixed trims ranging from 10° to 23° in order to obtain trims of approximately 6° and 15° with respect to the inclined water surface. These trims were chosen so that the data of this paper could be directly compared with smooth-water data (reference 4). The vertical velocities used varied from 0 to 11 feet per second which, together with horizontal velocities of 20 to 50 feet per second, resulted in flight-path angles ranging up to about 20°. Time histories of these velocities, horizontal and vertical displacements, and vertical accelerations were recorded for each run. A force, simulating wing lift, sufficient to support the 1230-pound dropping weight was applied to the float during impact by the lift (buoyancy) engine described in reference 3.

METHOD OF ANALYSIS

In reference 5 a generalized theoretical investigation of the loads and motions experienced by a seaplane in a step-landing impact showed that the hydrodynamic load can be represented in nondimensional form by means of the load-factor coefficient:

$$C_l = \frac{n_{i_v} g}{V_{v_0}^2} \left\{ \frac{W}{g} \frac{6 \sin \tau \cos^2 \tau}{[f(\beta)]^2 \phi(A) \rho \pi} \right\}^{1/3} \tag{1}$$

Reference 5 also showed that the variation of C_l during an impact, including the maximum value reached, is determined by the magnitude of a dimensionless approach parameter

$$\kappa = \frac{\sin \tau}{\sin \gamma_0} \cos(\tau + \gamma_0) \tag{2}$$

which may be considered a criterion of impact similiarity and which completely defines the nondimensional motion characteristics of an impact.

The functions $\phi(A)$ and $f(\beta)$ used in equation (1) are defined, for the purposes of this paper, as

$$\phi(A) = 1 - \frac{\tan \tau}{2 \tan \beta}$$

and

$$f(\beta) = \frac{\pi}{2\beta} - 1$$

The numerical values of these functions are in agreement with experimental results for the range of dead-rise angles between $22\frac{1}{2}^\circ$ and 30°. (See references 4 to 6.)

Equations (1) and (2) may be applied to the rough-water case if the initial conditions of the impact are defined relative to an inclined plane simulating the wave surface (references 1 and 2). In order for this inclined plane to be equivalent to the actual wave surface, its angle of inclination must be such that impacts at the same flight conditions into either surface will result in the same maximum load factor. Equations (1) and (2) may be rewritten, relative to the inclined-plane surface, as

$$C_{l_e} = \frac{n_{i_n} g}{V_{v_{e_o}}^2} \left\{ \frac{W}{g} \frac{6 \sin \tau_e \cos^2 \tau_e}{[f(\beta)]^2 \phi(A_e) \rho \pi} \right\}^{1/3} \tag{3}$$

and

$$\kappa_e = \frac{\sin \tau_e}{\sin \gamma_{e_o}} \cos\left(\tau_e + \gamma_{e_o}\right) \tag{4}$$

The only differences between equations (3) and (4) and equations (1) and (2) are the inclination of the surface through which the impact takes place and increments of velocity due to motion of the water. The two equations of each set are thus related by the same function, which is represented by the theoretical line in figure 7.

The quantities which must be redefined to fit the rough-water case, represented by equations (3) and (4), are trim, direction of load, velocity, and flight-path angle. Thus, if θ is the angle of inclination of the water surface,

$$\tau_e = \tau - \theta \tag{5}$$

and since the resultant load is in a direction substantially normal to the keel and only the vertical component was measured,

$$n_{i_n} = n_{i_r} \cos \tau_e = \frac{n_{i_v} \cos \tau_e}{\cos \tau} \tag{6}$$

Investigation of the proper method of introducing the increments of velocity due to wave motion revealed several recognized assumptions, three of which were finally considered. The first and most nearly correct of these assumptions (references 7 and 8) uses the orbital velocities of the water particles and would involve integration of velocities over the wetted area of the float and along the path through the water, a refinement which is not warranted by the accuracy of the other measurements of the tests. The second assumption (reference 9) considers that the velocity to be used is normal to the inclined water surface and of a magnitude equal to the normal component of the wave velocity. The third and simplest assumption (reference 2) treats the wave as a body of water in horizontal translation at the wave velocity.

A preliminary analysis of the data indicated that use of the slope at the point of contact, as in reference 2, did not give good results for all wave conditions or all points of contact. Trial-and-error solutions of equations (3) and (4) were therefore made to determine the equivalent slope for each run. This equivalent slope is the angle of inclination of a plane water surface by which the wave surface could be replaced without changing the resulting maximum normal impact load factor for a given impact. The solutions were made using both the second and third assumptions on wave velocity and the results of the solutions are shown as test points in figures 5 and 6, respectively. Examination of these two figures reveals that the second or normal-velocity method results in slopes as much as 30 percent higher than the maximum actual or trochoidal slopes while the third or horizontal-velocity method results in maximum equivalent slopes of about the same magnitude as the maximum actual or trochoidal slopes. Since the maximum equivalent slopes should be about the same as or slightly less than the maximum slopes of the waves used, the horizontal-velocity method of including wave motion appears to give results which are more accurate and consistent than results given by the normal-velocity method.

By use of the assumption that the wave is a body of water in horizontal translation, the float motion is referred to the wave. The relative horizontal velocity then becomes

$$V_h = V_{f_h} + V_w$$

The float velocity normal to the inclined water surface is

$$V_{v_{e_o}} = V_{f_v} \cos \theta + \left(V_{f_h} + V_w \right) \sin \theta \tag{7}$$

and the flight-path angle relative to the water surface is

$$\gamma_e = \theta + \gamma_r = \theta + \tan^{-1} \frac{V_{f_v}}{V_{f_h} + V_w} \qquad (8)$$

The wave velocity used in this paper is the measured velocity of the test waves. The wave slopes used will be discussed subsequently.

RESULTS AND DISCUSSION

The test conditions, which give the attitude and motion of the model at the instant of initial contact with the water, the point of contact of the float along the wave, and the wave condition used for the test, are presented in table II. The maximum values of measured load factor and computed values of several resulting quantities are also presented in table II and are shown in figures 7 to 11. These quantities may be considered to apply to V-bottom floats with an angle of dead rise of 30° in step landings in rough water when the effects of an afterbody and freedom of trim are small.

The wave profiles shown in figure 4 do not represent any particular wave but are the average of a number of profiles of individual waves obtained by photographic observation. The scatter of these individual wave profiles was less than the difference between the average wave and a trochoidal profile of the same dimensions. Also, since the average profiles do not differ greatly from the trochoidal profiles, as shown in figure 4, no appreciable loss of accuracy is introduced by the use of trochoidal profiles throughout the analysis.

The point of contact of the float along the wave profile was found by determining the height above the trough of the wave at which contact occurred. This height was determined by obtaining the vertical distance between the known initial position of the float and the trough of the wave and subtracting from it the measured displacement of the float at contact with respect to the same initial position. This result was checked by making a similar computation for the point of exit from the water and then comparing the recorded travel through the water with the horizontal distance between the computed points of contact and exit.

Calculation of Rough-Water Loads

In order to permit the calculation of rough-water loads by use of equations (3) and (4), a method must be found for determining the

equivalent slope from the parameters or characteristics of the waves involved. In reference 2 the assumption was made that this slope could be approximated by the angle of the water surface at the point of first contact of the float and the wave, which would be the case only when the ratio of wave length to float length is very large. Figure 6 shows that this assumption holds approximately for relatively small ratios when the contact occurs on certain portions of the wave profile, such as those used in reference 2, but does not hold for contacts on all portions of the wave.

This assumption is further illustrated by figure 7. The experimental points in figure 7 were computed by use of the trochoidal slope at the point of contact for each run. Examination of these data together with those of figure 6 shows that the load-factor coefficients plotted in figure 7 lie above or below the theoretical line as the corresponding equivalent slopes of figure 6 lie above or below the curve of trochoidal slope. Further examination of figure 6 reveals that, although not identical, a definite relation exists between the equivalent-slope data and the curves representing actual or trochoidal slopes of the waves. This relation is best characterized as a phase offset between the curve of equivalent slope and the curve representing the slope of a trochoidal wave of the same dimensions. This phase offset could probably be taken into account by the use of a slope encountered at some point during the impact instead of at the point of first contact. However, an analysis of this aspect of the problem is beyond the scope of this investigation.

If only the critical loads are to be calculated, a much simpler approach to the problem can be made. The ratio of the measured normal load factor to the normal load factor predicted by use of equations (3) and (4) with an equivalent slope equal to the maximum positive slope $\left(\theta = \tan^{-1} \dfrac{\pi H}{L}\right)$ of a comparable trochoid is shown in figure 8 plotted against the position of contact along the wave. From the plot it may be seen that the ratio attains a value of about 1 at a station along the wave corresponding approximately to the position of the maximum slope and that at all other stations its value is less than 1. For this reason the calculated value of the load factor is a good approximation of the experimental value for impacts at the critical portion of the wave and is conservative for impacts at all other portions.

The effect of the ratio of wave length to float length on the load-factor ratio $n_{i_{n_m}}/n_{i_{n_{th}}}$ is shown in figure 9. The upper curve represents the maximum values of the data at each wave condition and the lower curve similarly represents the average of the highest 25 percent of the data. The curves on this plot indicate that for impacts in waves shorter than 5 float-forebody lengths the most severe loads do not attain the calculated maximum value. As the wave length becomes

greater with respect to the float size the experimental loads can be seen, however, to approach the calculated loads as indicated by the tendency of the lines to approach a value of 1 with about a 10-percent scatter.

Comparison with Smooth-Water Conditions

Figure 10 shows, for each run, the ratio of the vertical component of the maximum measured impact load factor to the maximum theoretical load factor which would be obtained at the same flight conditions but in smooth water. This ratio $n_{i_{v_m}}/n_{i_{v_{th}}}$ is plotted against flight-path angle γ_{h_o} relative to level water.

The test points lying near the envelope curve represent impacts having points of contact at or near the position of the maximum positive slope, while those scattered farther below the curve represent contacts at other points along the wave profile. Since the points near the curve represent impacts at various wave conditions and trims, the curve represents a variation with flight-path angle as the only important variable.

It can be seen from the figure that the loads encountered in rough water can be as much as eight times the comparable smooth-water loads. However, these high values of load ratio occur at low flight-path angles and, therefore, represent small values of smooth-water load rather than large values of rough-water load. The largest loads actually were encountered at the high flight-path angles where, because of the large values of smooth-water loads, the load ratio reached a value of only 2.

The significance of this plot (fig. 10) lies in the small maximum values of load ratio which occur at large flight-path angles as compared with the values obtained at small flight-path angles. These small values indicate that design criterions based on impacts into smooth water at flight-path angles above about 12° could be used for rough-water designs by using a safety factor of only 2.

Equations (3) and (4) have shown that the loads imposed on a given float during impacts in rough water will be determined by velocity, flight-path angle, and trim referred to the wave surface. The slope of the inclined-plane water surface can therefore vary without affecting the loads as long as these three flight quantities remain constant. This fact is illustrated by figure 11 and the data in table III. The data presented in table III were obtained from the data of table II of this paper and of table II of reference 4. They represent runs at two values of effective trim and roughly constant values of effective flight-path angle and effective velocity but with an equivalent slope which varies from 0° to about 14°. The choice of runs was further restricted

by holding the values of X/L within narrow limits, near the position of maximum equivalent slope. The equivalent slope used was the maximum trochoidal slope as used in figures 8 and 9. In addition, approximately average values of each of the flight conditions were obtained and were used to compute average load-factor values. In figure 11 the two computed load-factor values appear as horizontal lines, one for each effective trim. The scatter of the points is caused not only by the inaccuracies of experimental measurements but also by the unavoidable scatter of flight conditions. Figure 11 shows, however, no trend toward higher loads in steeper waves as long as the flight conditions are held constant with respect to the wave surface. An airplane which was designed for hard, high-flight-path-angle impacts in smooth water could therefore be used safely in rough-water impacts at low speeds and flight-path angles such as would be encountered in landing into waves and into a stiff head wind.

CONCLUSIONS

An analysis was made of experimental data for fixed-trim impacts in advancing waves of a prismatic-float forebody 10 feet in length and having an angle of dead rise of 30°. The waves used were about 2 feet in height and 60, 45, or 30 feet in length. The analysis has resulted in the following conclusions for impacts under these conditions:

1. If the maximum slope of a comparable trochoid is used in the hydrodynamic-load equation for the calculation of rough-water loads, the calculated values of maximum load agree with the measured loads within 10 percent for waves longer than 5 float-forebody lengths.

2. A relationship exists between the wave slope and the slope of an equivalent inclined-plane water surface for any point of contact.

3. Airplanes designed for hard, high-flight-path-angle impacts in smooth water can be used safely for landings in rough water at low speeds and flight-path angles.

Langley Aeronautical Laboratory
     National Advisory Committee for Aeronautics
          Langley Field, Va., September 23, 1948

REFERENCES

1. Mayo, Wilbur L.: Analysis and Modification of Theory for Impact
     of Seaplanes on Water. NACA Rep. No. 810, 1945.

2. Milwitzky, Benjamin: A Theoretical Investigation of Hydrodynamic
     Impact Loads on Scalloped-Bottom Seaplanes and Comparisons with
     Experiment. NACA TN No. 1363, 1947.

3. Batterson, Sidney A.: The NACA Impact Basin and Water Landing Tests
     of a Float Model at Various Velocities and Weights. NACA Rep.
     No. 795, 1944.

4. Miller, Robert W., and Leshnover, Samuel: Hydrodynamic Impact
     Loads in Smooth Water for a Prismatic Float Having an Angle of
     Dead Rise of 30°. NACA TN No. 1325, 1947.

5. Milwitzky, Benjamin: A Generalized Theoretical and Experimental
     Investigation of the Motions and Hydrodynamic Loads Experienced
     by V-Bottom Seaplanes during Step-Landing Impacts. NACA TN
     No. 1516, 1948.

6. Mayo, Wilbur L.: Theoretical and Experimental Dynamic Loads for

     a Prismatic Float Having an Angle of Dead Rise of $22\frac{1}{2}°$. NACA RB
     No. L5F15, 1945.

7. Beach Erosion Board: A Summary of the Theory of Oscillatory Waves.
     Tech. Rep. No. 2, Off. of Chief of Engineers, War Dept., 1942.

8. Taylor, D. W.: The Speed and Power of Ships. Ransdell Inc.
     (Washington, D. C.), 1933, pp. 5-11.

9. Hedrick, I. G., and Siebert, E. G.: Water Loads Investigation - Air-
     plane Model XJR2F-1. Rep. No. 2903.41, Grumman Aircraft Eng. Corp.,
     May 19, 1946.

TABLE I. - OFFSETS OF LANGLEY IMPACT-BASIN FLOAT MODEL M-2 (SEE FIG. 1)

[All dimensions are in inches]

| Station	Half-breadth		Height above datum line			
	Upper and lower chine	Deck	Keel	Upper chine	Lower chine	Deck
0	0	0.33	23.05	25.26	23.05	32.28
2	2.15	1.45	16.25	25.71	21.04	32.85
5	4.25	3.05	12.52	26.53	22.70	33.49
9	7.80	4.58	9.52	26.32	23.41	34.19
14	10.31	5.93	6.94	24.47	22.18	34.77
21	12.81	7.23	4.47	21.62	19.44	35.20
29	15.09	8.15	2.60	19.36	16.55	35.27
38	16.86	8.71	1.24	16.41	13.64	35.27
47	18.04	8.94	.40	14.54	11.62	35.27
58	18.87	9.00	0	12.90	10.70	35.27
72	19.33	9.00	0	11.58	10.96	35.27
87.25	19.40	9.00	0	11.18	10.99	35.27
106.625	19.40	9.00	0	11.18	10.99	35.27
120.75	19.40	9.00	0	11.18	10.99	35.27

NACA
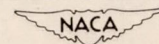
TABLE II

TEST DATA AND RESULTS FOR ROUGH-WATER IMPACTS

Run number	τ (deg)	n_{1v_m} (g)	$v_{f_{v_0}}$ (fps)	$v_{f_{h_0}}$ (fps)	γ_{h_0} (deg)	$\frac{X}{L}$	θ_{th} (deg)	c_{l_e}	κ_e	$\frac{n_{1n_m}}{n_{1n_{th}}}$	$\frac{n_{1v_m}}{n_{1v_{th}}}$
				L = 60; H = 1.85; V_w = 14.00							
1	10	1.68	2.61	44.4	3.36	0.700	3.1	0.917	0.668	0.678	3.02
2		1.90	3.79	40.5	5.35	.612	3.0	1.465	.946	.686	2.30
3		2.48	2.02	44.1	2.62	.810	5.6	1.617	.993	1.071	5.73
4		2.60	2.81	47.1	3.41	.696	4.5	1.558	1.062	.882	3.75
5		3.07	2.87	47.8	3.44	-----	---	-----	-----	-----	4.24
6	13	3.36	3.00	48.3	3.55	.828	6.0	1.711	.967	1.072	4.35
7		2.79	5.35	47.6	6.41	.644	2.1	1.281	1.023	.644	1.80
8		3.45	6.07	50.5	6.85	-----	---	-----	-----	-----	1.81
9		2.65	9.08	30.7	16.48	.642	-1.2	1.262	.767	.556	1.13
10		6.18	11.10	31.3	19.53	-----	---	-----	-----	-----	1.94
11		.83	1.89	22.2	4.86	.627	2.8	2.559	2.482	.662	3.06
12		2.60	3.46	40.3	4.91	.637	4.0	2.688	2.113	.842	2.89
13		1.91	3.66	35.1	5.95	.637	2.6	2.052	1.942	.693	2.21
14	21	1.86	4.70	30.3	8.82	.684	1.0	1.349	1.361	.668	1.81
15		1.99	7.57	24.0	17.51	.925	-1.2	1.109	1.064	.576	1.24
16		2.21	7.77	24.1	17.87	.695	-.6	.905	.837	.626	1.32
17		1.16	7.77	23.0	18.67	.250	-5.5	3.940	3.517	.338	.72
				L = 45; H = 2.16; V_w = 13.15							
18		0.35	0	29.2	0	0.833	2.4	0.340	0.802	0.240	----
19		.70	1.96	37.5	2.99	.876	.8	.351	.738	.240	1.79
20		2.40	2.02	36.8	3.14	.722	7.0	1.126	.681	.836	6.06
21		3.28	2.81	39.6	4.06	.704	8.0	1.379	.725	.928	5.15
22		.50	2.94	40.5	4.15	.911	-1.1	.268	.937	.135	.73
23		3.95	3.53	40.7	4.96	.709	8.1	1.306	.634	.977	4.61
24		3.40	3.72	41.7	5.10	.740	6.4	.950	.560	.801	3.66
25		1.15	2.87	30.8	5.32	.842	2.1	.512	.567	.427	2.17
26	15	.15	3.07	31.9	5.52	.156	-2.9	-----	-----	.052	.25
27		1.80	3.72	31.4	6.76	.667	3.1	.922	.726	.576	2.41
28		4.89	6.33	40.7	8.84	.753	6.9	.891	.428	.863	2.77
29		5.18	6.60	41.7	8.99	.700	6.3	1.068	.519	.868	2.75
30		2.58	6.79	40.5	9.52	.628	.6	.797	.760	.436	1.35
31		4.20	8.23	42.3	11.01	.758	2.6	.568	.372	.590	1.66
32		5.50	8.16	40.9	11.28	.658	8.7	1.134	.570	.799	2.22
33		.50	0	20.8	0	.793	4.2	.953	1.559	.466	----
34		1.30	2.81	41.7	3.86	.882	1.1	.717	1.438	.317	1.80
35		3.64	3.40	40.7	4.78	.751	6.8	1.442	1.116	.852	4.07
36		3.02	3.40	40.0	4.86	.678	4.5	1.492	1.434	.642	3.42
37		3.53	3.53	41.2	4.90	.682	6.2	1.773	1.365	.797	3.78
38	23	3.03	3.53	36.8	5.48	.667	6.0	1.880	1.426	.789	3.46
39		2.65	3.72	30.8	6.89	.704	6.2	1.544	1.154	.820	3.61
40		.77	4.05	23.5	9.78	.349	-1.4	-----	-----	.296	1.08
41		1.40	4.05	23.2	9.90	.838	2.1	.825	.910	.547	1.97
42		1.12	3.98	22.4	10.08	.853	.8	.710	.932	.456	1.65
43		1.49	4.18	21.7	10.90	.722	2.8	.922	.900	.599	2.12
44		1.06	4.57	23.4	11.05	.460	-.2	5.051	3.906	.382	1.28
45		2.35	6.53	22.8	15.98	.698	3.0	.961	.757	.673	1.84
				L = 30; H = 2.30; V_w = 11.31							
46		2.35	1.70	30.2	3.22	0.766	9.7	0.628	0.309	0.665	8.18
47		.52	2.87	36.5	4.49	.930	-.2	.183	.444	.098	.80
48		4.20	3.40	40.7	4.78	.763	10.6	.637	.303	.651	4.88
49	18	3.46	3.00	35.7	4.80	.750	10.0	.674	.320	.153	4.89
50		.67	3.00	31.0	5.52	.827	-.4	.118	.215	.153	1.12
51		2.48	3.33	30.8	6.17	.783	7.3	.470	.247	.548	3.70
52		6.23	6.14	41.7	8.38	.623	10.0	1.767	.774	.716	2.12
53		5.50	7.84	41.2	10.77	.613	6.5	1.260	.711	.548	2.28

NACA
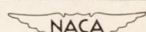
TABLE III

COMPARISON OF EFFECTIVE CONDITIONS AT VARIOUS WAVE SLOPES

Run number	θ (deg)	τ_e (deg)	γ_{e_0} (deg)	$V_{v_{e_0}}$ (fps)	$n_{i_{n_m}}$ (g)
[a]3	0	6.00	14.42	9.27	2.59
7	5.53	7.47	10.49	11.27	3.51
27	8.57	6.43	13.34	10.32	1.85
46	13.54	4.46	15.89	11.37	2.46
Representative value:		6.00	15.00	10.00	2.88
[a]9	0	15.00	16.29	9.43	2.52
16	5.53	12.47	17.06	11.40	2.28
45	8.57	14.43	18.86	11.82	2.47
Representative value:		15.00	15.00	10.00	3.03
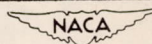
[a] Data from smooth-water run from reference 4.
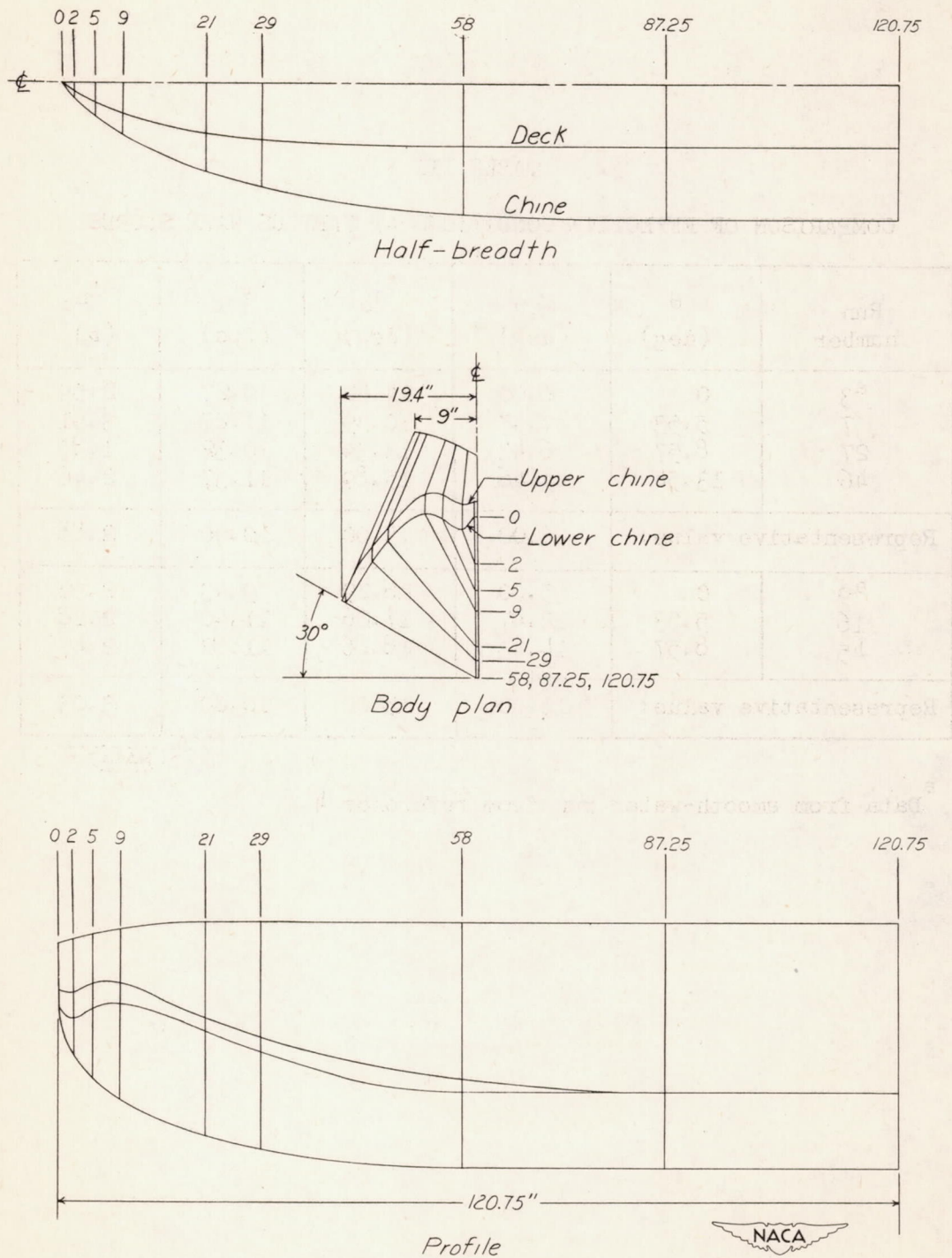
Figure 1.- Lines of Langley impact-basin float model M-2.
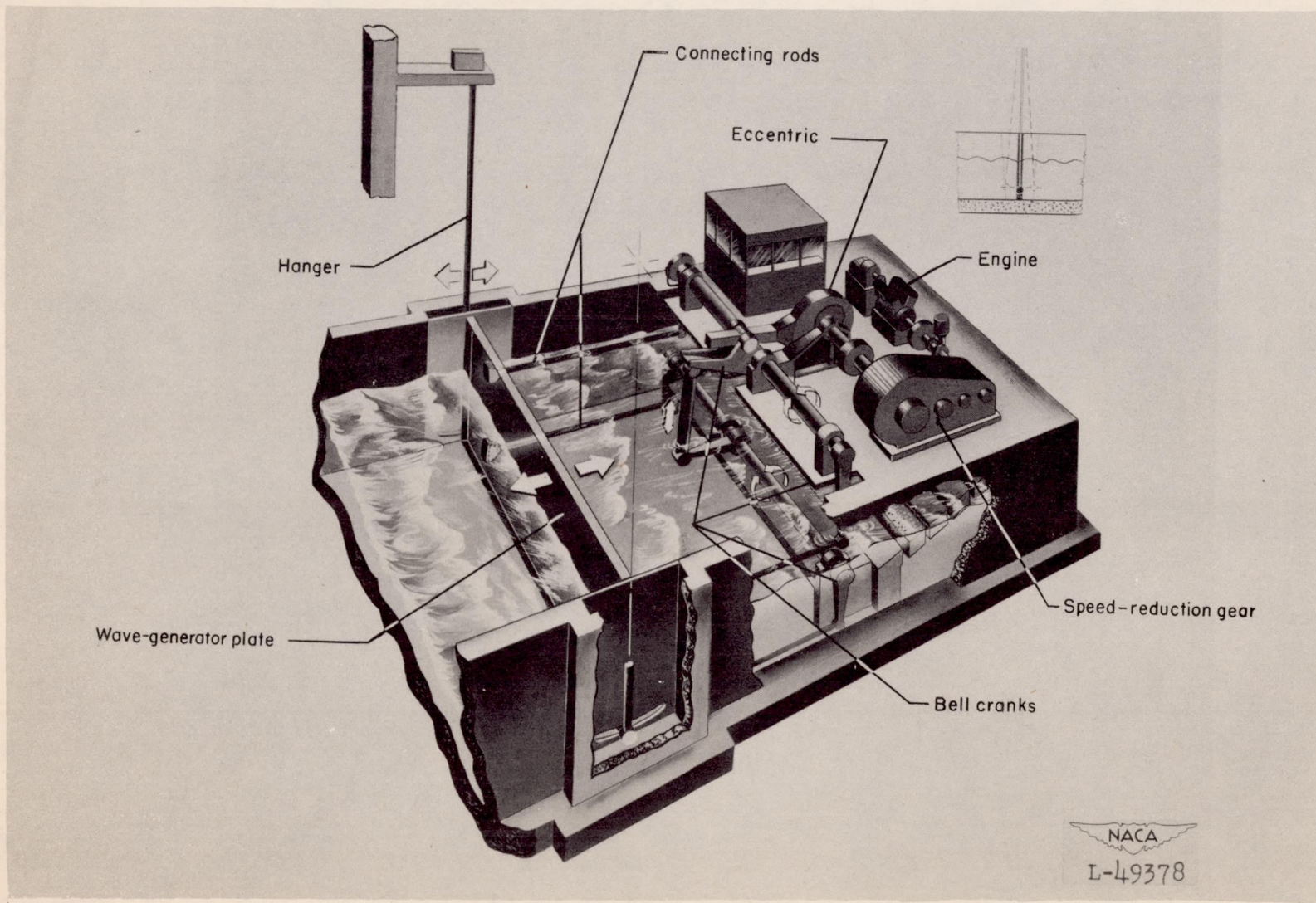
Figure 2.- Sketch of Langley impact-basin wave maker.
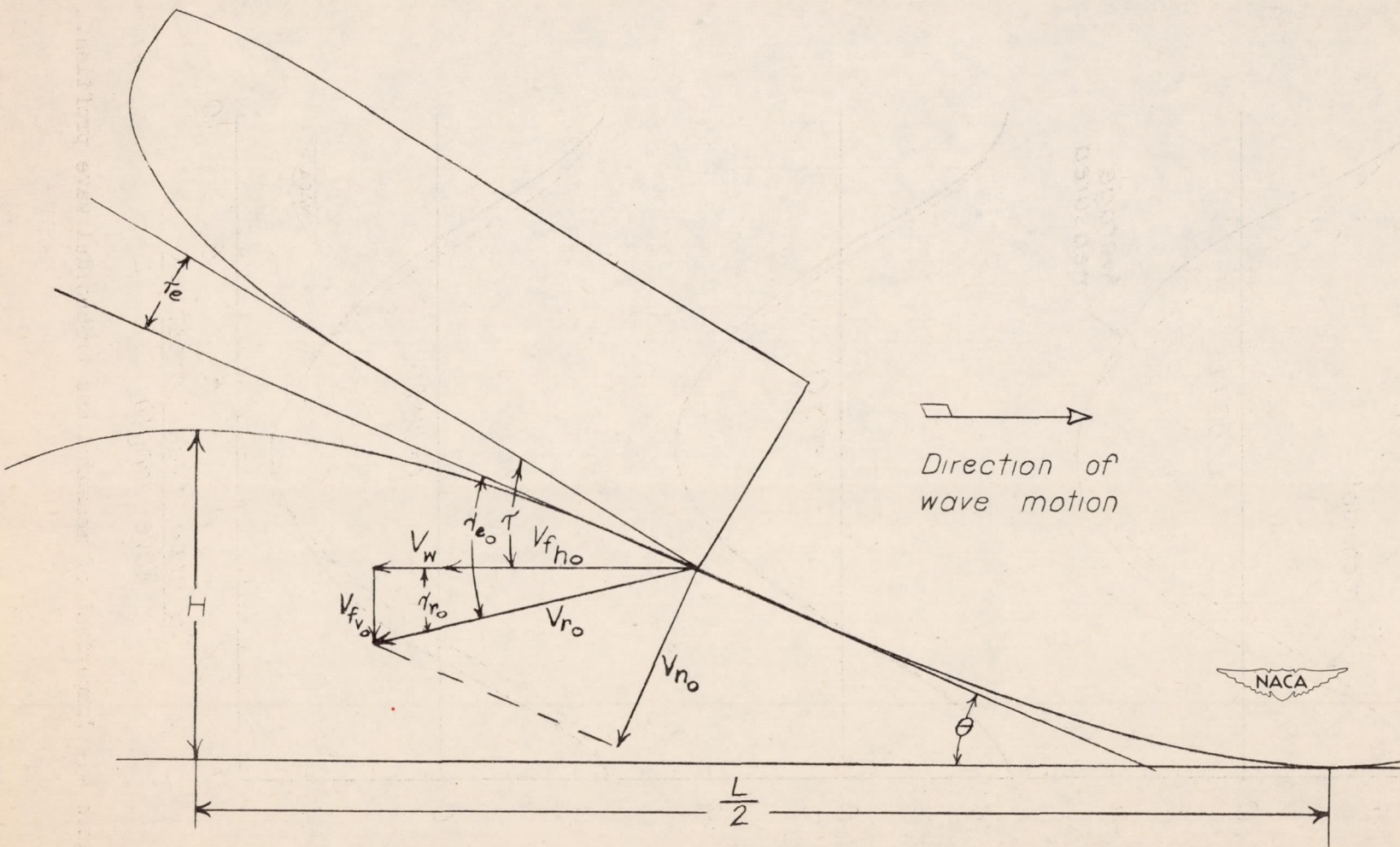
Figure 3.- Velocities and angles at contact on wave.
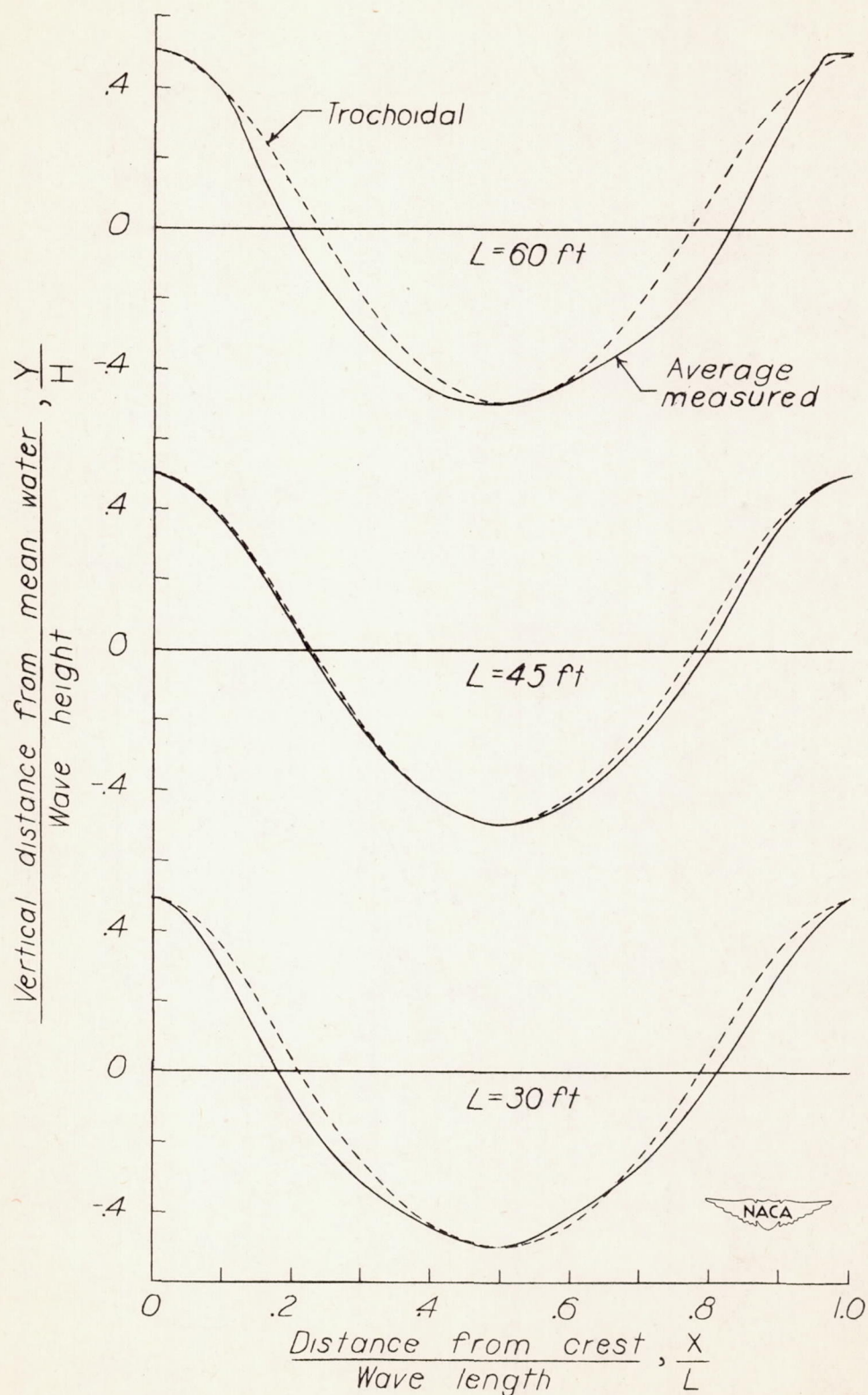
Figure 4.- Comparison of measured and trochoidal wave profiles.
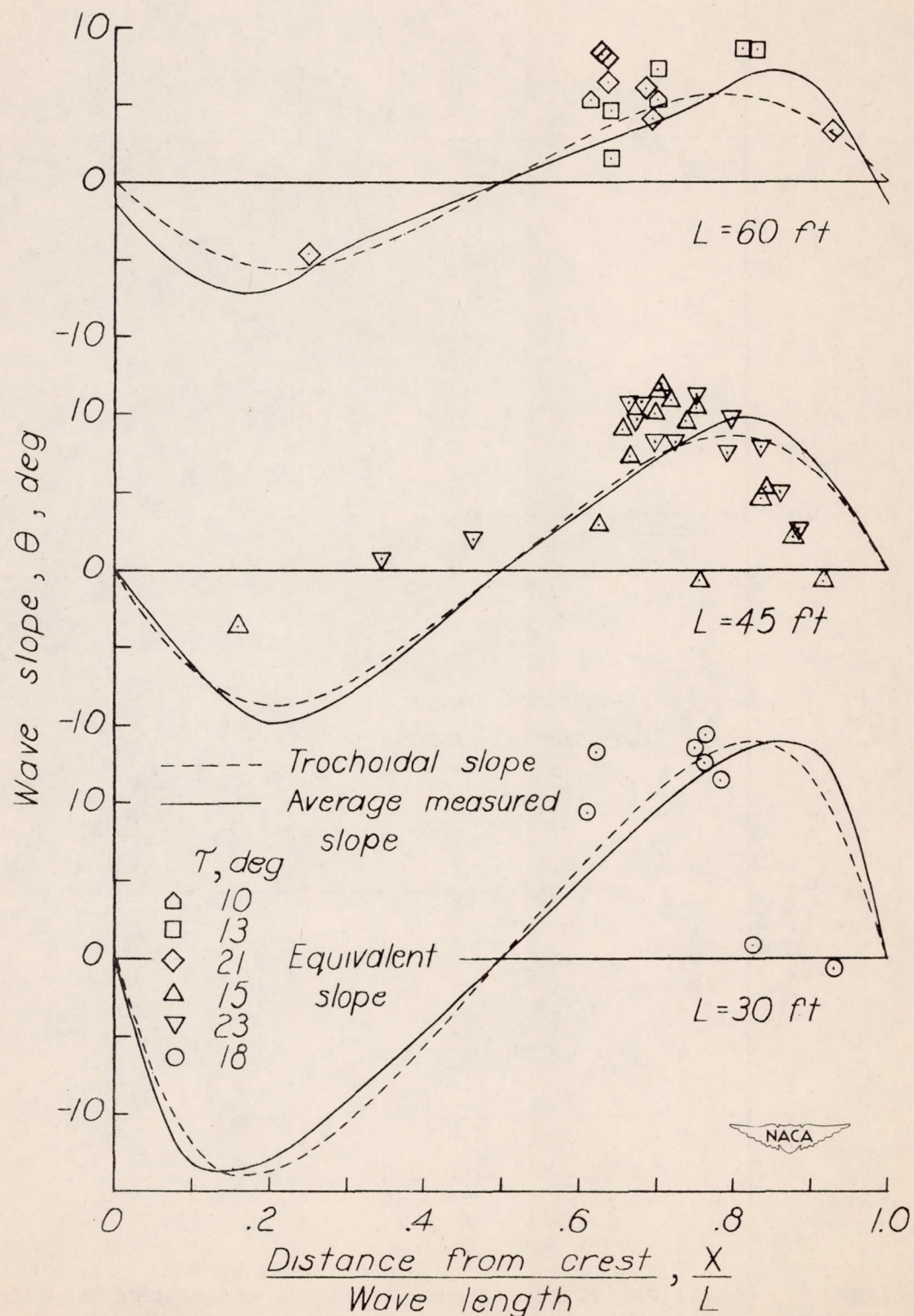
Figure 5.- Comparison of equivalent, measured, and trochoidal wave
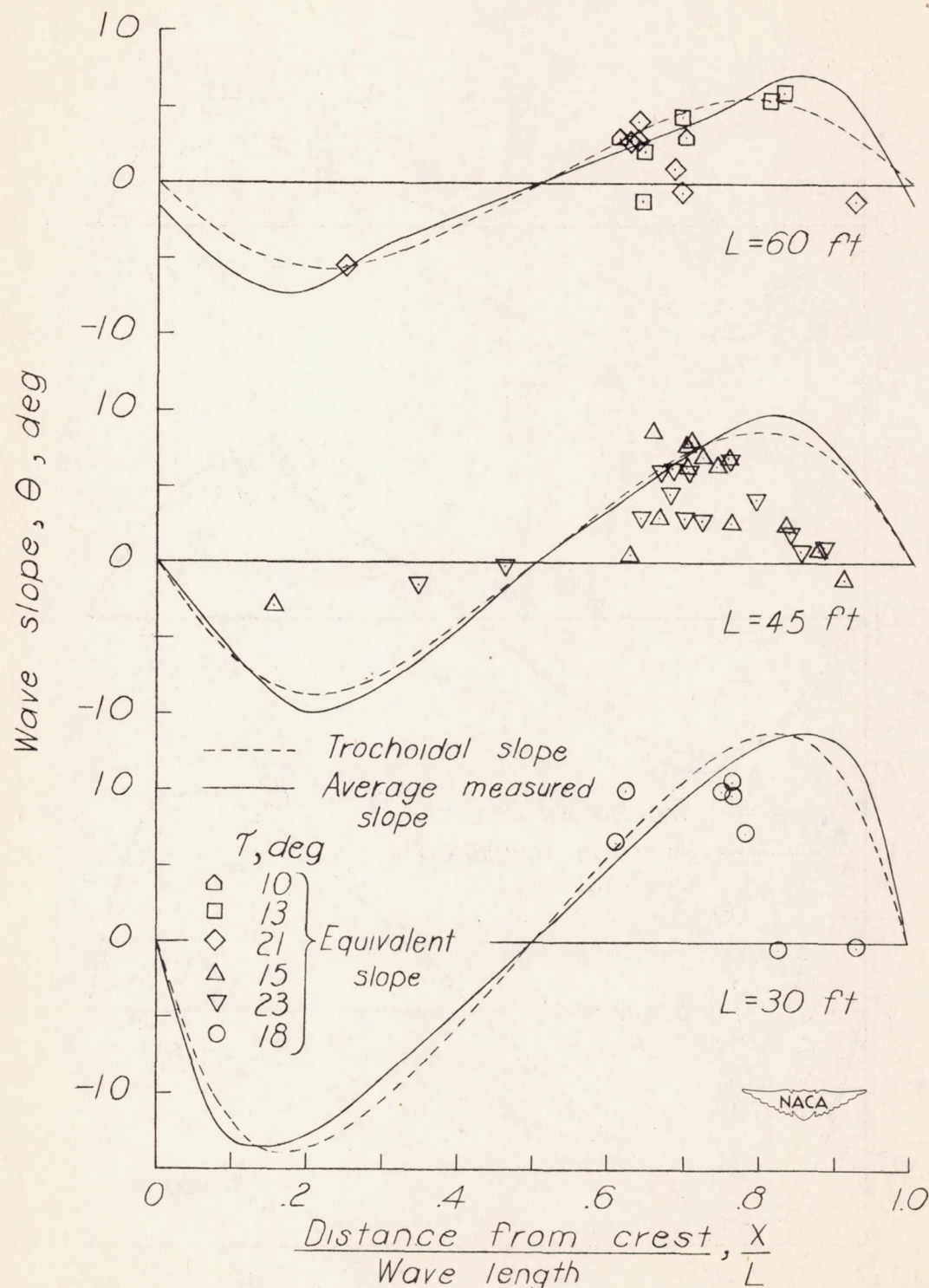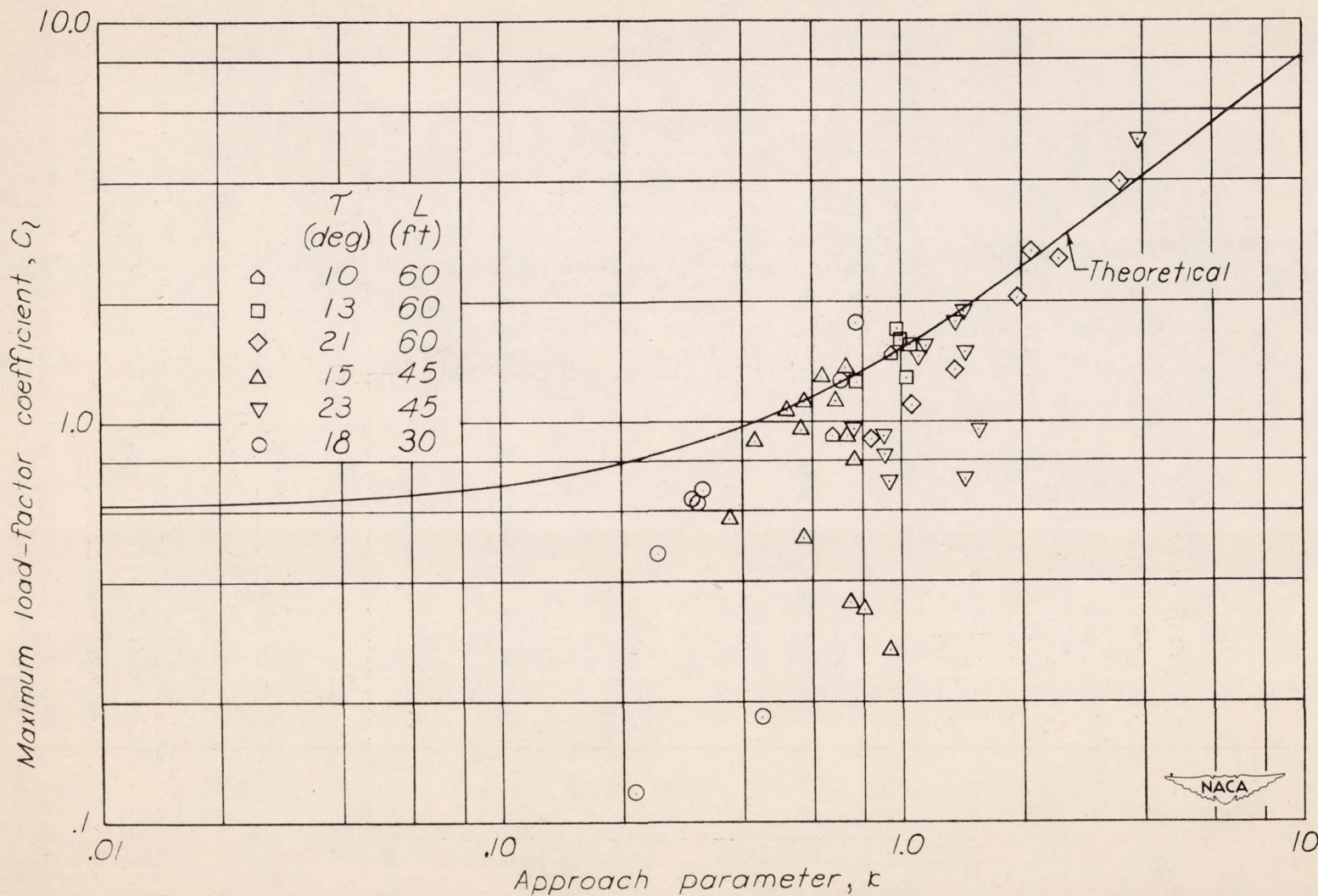slopes. Equivalent slopes computed using wave normal velocity.

Figure 6.- Comparison of equivalent, measured, and trochoidal wave
    slopes. Equivalent slopes computed using wave horizontal
    velocity.

Figure 7.- Variation of maximum load-factor coefficient with approach parameter. θ, trochoidal slope at point of contact.
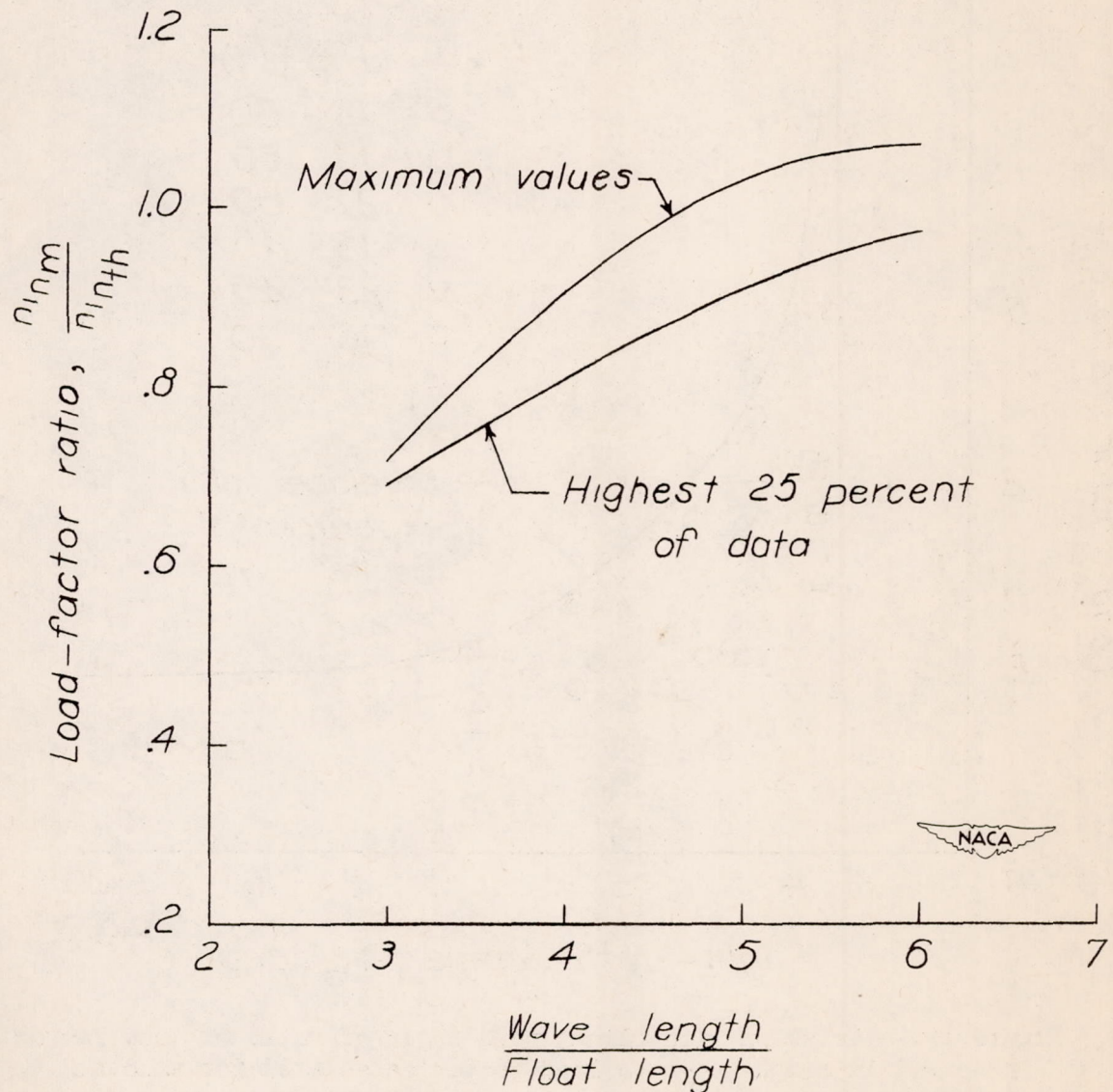
Figure 9.- Variation of load-factor ratio (measured normal load factor to theoretical normal load factor) with ratio of wave length to float length. Theoretical slope, $\theta = \tan^{-1} \frac{\pi H}{L}$.
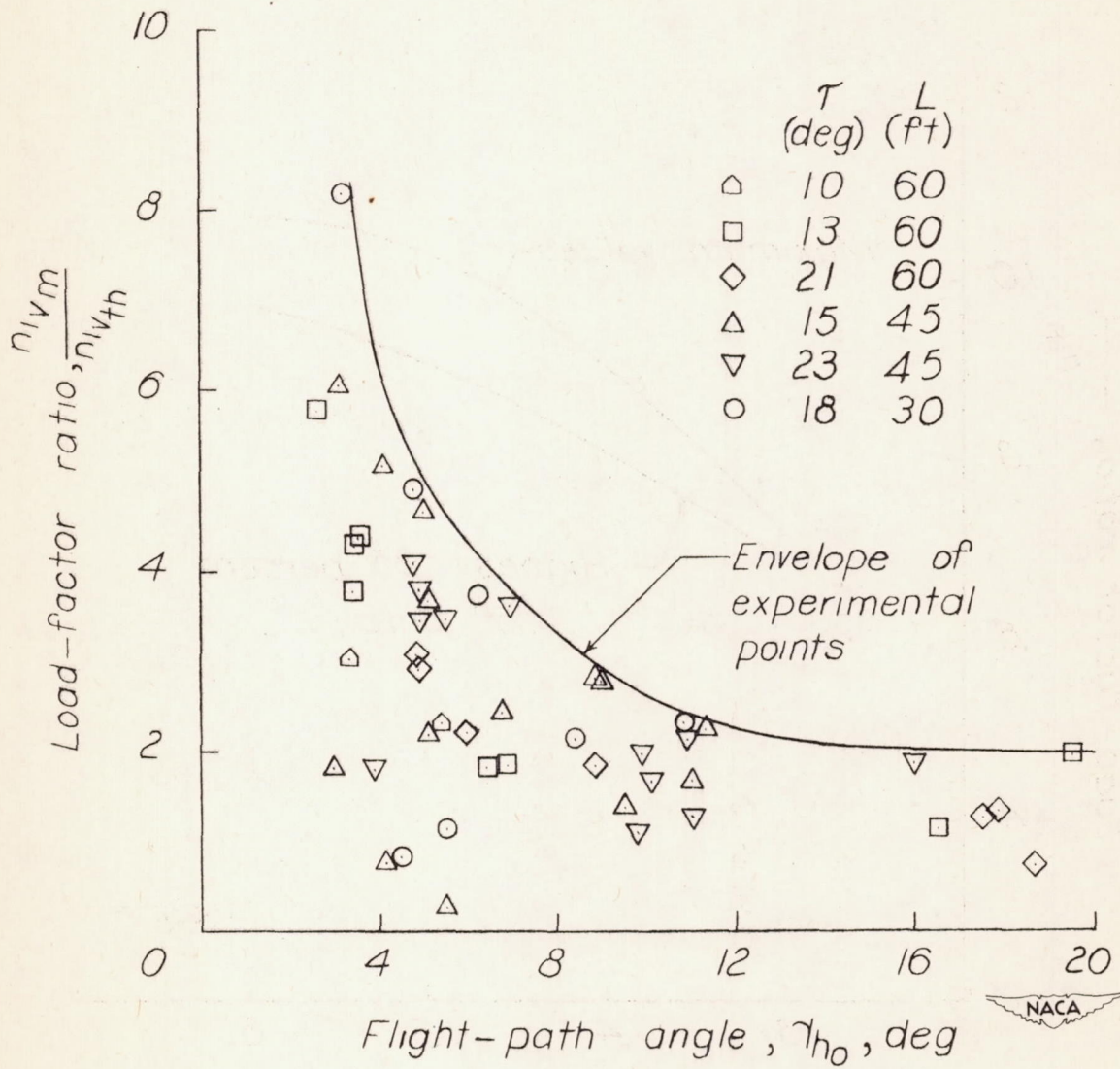
Figure 10.- Variation with flight-path angle of ratio of load factor
    measured in rough water to load factor calculated for smooth
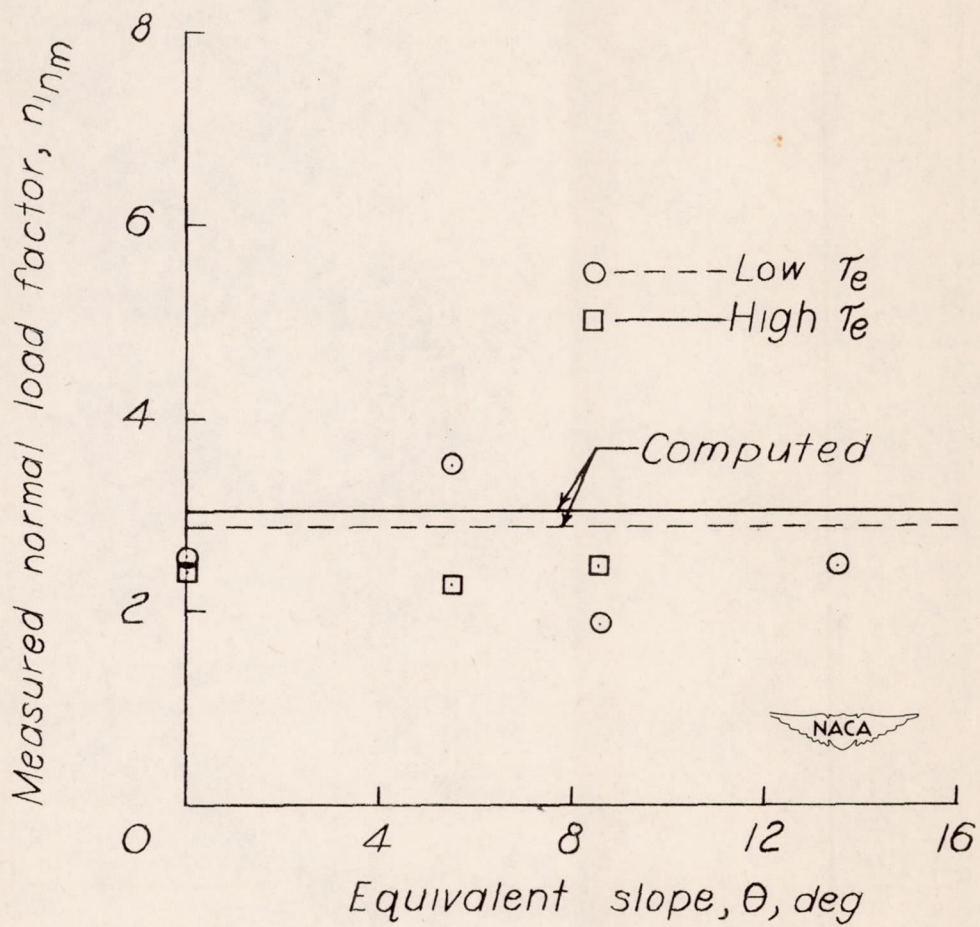   water.

Figure 11.- Variation of normal measured load factor with equivalent slope. $\theta = \tan^{-1} \frac{\pi H}{L}$.